Journal Pre-proofs

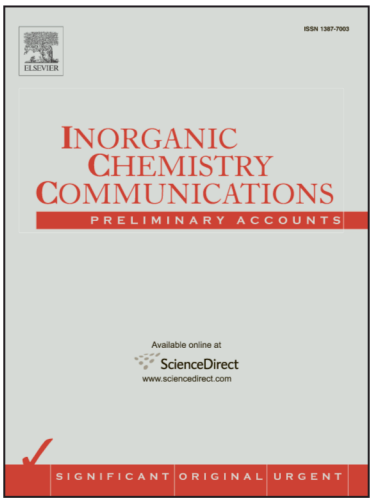

Short communication

New cobalt(II) Schiff base complex: synthesis, characterization, DFT calculation and antimicrobial activity

Jian-Hong Jiang, Yan-Hua Lei, Xu Li, Yiyuan Pi, He Zhu, Qiang-Guo Li, Chuan-Hua Li

PII: S1387-7003(20)30940-0
DOI: https://doi.org/10.1016/j.inoche.2020.108350
Reference: INOCHE 108350

To appear in: *Inorganic Chemistry Communications*

Received Date: 26 August 2020
Revised Date: 15 November 2020
Accepted Date: 18 November 2020

Please cite this article as: J-H. Jiang, Y-H. Lei, X. Li, Y. Pi, H. Zhu, Q-G. Li, C-H. Li, New cobalt(II) Schiff base complex: synthesis, characterization, DFT calculation and antimicrobial activity, *Inorganic Chemistry Communications* (2020), doi: https://doi.org/10.1016/j.inoche.2020.108350

New cobalt(II) Schiff base complex: synthesis, characterization, DFT calculation and antimicrobial activity

Jian-Hong Jiang, Yan-Hua Lei, Xu Li, Yiyuan Pi, He Zhu, Qiang-Guo Li, Chuan-Hua Li*

Hunan Provincial Key Laboratory of Xiangnan Rare-Precious Metals Compounds and Applications, College of Chemical Biology and Environmental Engineering, Xiangnan University, Chenzhou 423043, Hunan Province, P.R. China.

*Corresponding author. Tel./Fax: +86-735-2653353
E-mail address: lichuanhua0526@126.com (C.-H. Li)

Abstract

A new cobalt(II) Schiff-base complex [$Co(L)_2$] was prepared by using equivalent molar of Schiff-base ligand [HL=(E)-N'-(2-hydroxy-3-methoxybenzylidene)isonicotinohydrazide] and $CoCl_2$•$6H_2O$. The structure of the complex was characterized by single-crystal X-ray diffraction, IR, ESI-MS, elemental analysis and DFT method. X-ray crystal structure analysis showed that the complex crystallized in space group Pbca, with two symmetry-independent molecules. The experimental vibrational bands(IR) have been discussed and assigned based on DFT calculations. The antibacterial activity of Schiff base and its complex against S. pombe were assessed by bio-microcalorimetry at 32 °C. Some thermokinetic parameters (k, $P_{max,}$ t_G and Q_{total}) were derived from the metabolic power–time curves, and their quantitative relationship with the concentration were analyzed. The half inhibition concentration (IC_{50}) of Schiff base and its complex were calculated to be 1.18×10^{-2} mol L^{-1} and 1.07×10^{-3} mol L^{-1}, respectively. The inhibition effect of the complex showed much stronger than that of Schiff base.

Keywords: Isoniazid; Schiff base; Cobalt(II) complex; DFT calculations; Bio-microcalorimetry; Thermokinetic parameters

1. Introduction

Schiff base is a class of organic compound containing an azomethine (-HC=N-) or imine (>C=N-) group, which is usually formed by condensation of active carbonyl group (aldehyde or ketone) with a primary amine under azeotropic distillation [1]. Over the years, the coordination chemistry of Schiff bases has received much attention of researchers due to their flexible coordination modes and multiple metal coordination behaviors. Complexes constructed by Schiff bases possess important medicinal properties such as antimicrobial, antibacterial, antifungal and anticancer activity [2-6]. Isoniazid (also, Nicotinic Acid Hydrazide, INH or H) was known as early as 1912 [7]. The appearance of Isoniazid has been regarded as a very important milestone in the history of the conquest of tuberculosis. Isoniazid, along with rifampicin (RIF), ethambutanol (EMB), pyrazinamide (PZA) and streptomycin, has been identified by World Health Organization(WHO) as the first-line antitubercular drug [8]. The function of isoniazid is to inhibit the production of Mycolic Acid, which is an essential cell wall component in tuberculosis [9].

In recent years, there has been also considerable interest in the chemistry of isoniazid Schiff bases and their complexes. Isoniazid, possessing an amino group, can react with various carbonyl compounds (aldehydes and ketones) to form Schiff bases (hydrazones), containing the characteristic H-C=N-NH- group. There is a possibility of tautomerism between the carbonyl group and the amino group in isoniazid Schiff base moiety in some cases [10]. Compared with the -C=N group, the presence of OH or NH groups in an appropriate position have greater chance to increase intramolecular as well as intermolecular interactions [11]. This indicates that isoniazid Schiff base may display much stronger bioactivity owing to improved interactions with the binding sites. Some transition-metal complexes of isoniazid Schiff bases have been investigated such as Cu(II), Zn(II) and Mn(II) [12-14]. Cobalt(II) complexes of (E)-N'-(2-hydroxy-3-methoxybenzylidene)isonicotinohydrazide $[Co(HL)_2](NO_3)_2 \cdot 3H_2O$ has been described in previous literature [15]. In this study, in continuation of our research on the on synthesis of Schiff base and their complexes [16-19], we have described the synthesis and characterization of new cobalt(II) complex of Schiff base derived from 3-methoxysalicylaldehyde with isoniazid (Scheme 1). The determinations of the X-ray structure of the complex and DFT calculations on it have been undertaken. The antibacterial activity of Schiff base and its cobalt(II) complex against S. pombe was investigated.

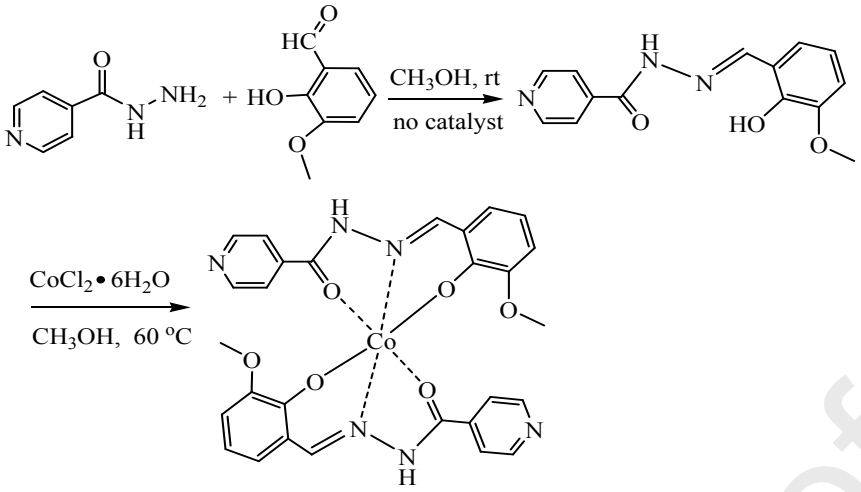

Scheme 1 Synthesis of cobalt(II) complex.

2. Experimental

2.1. Chemicals and physical measurements

3-Methoxysalicylaldehyde and isoniazid with analytical grade were purchased from Thermo Fisher Scientific. Other chemicals were purchased from the Sinopharm Chemical Reagent Co., Ltd. (Shanghai, China) and used without further purification. (E)-N'-(2-hydroxy-3-methoxybenzylidene)isonicotinohydrazide was prepared according to the published literature [14]. Schizosaccharomyces pombe (S. pombe) (ACCC 20047) was bought from Beijing Century Aoke Biological Technology Co., Ltd. YES medium (per liter) consisted of yeast (5.000 g), glucose (30.000 g), L-leu (0.225 g), L-lys (0.225 g), L-his (0.225 g), adenine (0.225 g), and uracil (0.225 g).

Carbon, hydrogen, and nitrogen analyses were determined using an elemental analyzer (Perkin-Elmer 2400 II). FT-IR spectra was measured with KBr discs on an Avatar 360 (Nicolet, Madison, USA) spectrophotometer in the wavenumber range of 4000–400 cm^{-1} with an average of 32 scans and 4 cm^{-1} of spectral resolution. A microcalorimetric study was carried out on a 3116-2/3239 TAM Air calorimeter (Thermometric AB, Sweden) [20]. Molecular weight of the complex was determined using a thermo TSQ Quantum Ultra Access triple-quadrupole mass spectrometer (Thermo Fisher Scientific, Waltham, MA). X-ray photoelectron spectroscopy (XPS) was measured on a Thermo Scientific Nexsa using monochromatized Al Kα radiation (1486.6 eV).

2.2. Synthesis of Schiff base

A mixture of isonicotinohydrazide (2 mmol, 0.274 g), 3-methoxysalicylaldehyde (2 mmol, 0.304 g) and methanol (25 mL) was allowed to stir for 2h without catalyst at room temperature.

The reaction mixture was concentrated on a rotary evaporator to the desired volume. The light yellow precipitate formed was collected by filtration under suction, washed repeatedly with methanol, and recrystallized twice with methanol. The pure product was dried at 60 ^{o}C in a vacuum oven, and then kept in a dessicator over anhydrous $CaCl_2$. Yield: 84%. The solid product was identified as $C_{14}H_{13}O_3N_3$. Spectroscopic data of Schiff base were given as follows: IR (KBr): 3024 cm^{-1} ($\nu_{C=C-H}$), 2840cm^{-1} (ν_{C-H}), 1690 cm^{-1} ($\nu_{C=N}$), 1603, 1567 cm^{-1} ($\nu_{C=C}$), 1464 cm^{-1} ($\delta_{as\ C-H}$), 1289 cm^{-1}, 1247 cm^{-1} (ν_{Ph-O}), 741 cm^{-1} . ^{1}H NMR(500MHz, DMSO-d6): δ 3.82 (s, 3H, CH_3O), 6.86-7.22 (3H, Ar), 7.84-7.85 (d, 2H, Ar), 8.70 (s, 1H, CH=N), 8.79-8.80 (d, 2H, Ar), 10.69(s, 1H, NH), 12.26 (s, 1H, OH). Elemental analysis for $C_{14}H_{13}O_3N_3$, Calc. (Found): C 61.99 (61.97), H 4.83 (4.80), N 15.49 (15.51) %.

2.3. Synthesis of the complex

A methanolic solution (5 mL) of $CoCl_2$•$6H_2O$ (0.5 mmol, 0.119 g) was added dropwise to a methanolic solution (20 mL) of Schiff base (0.5 mmol, 0.136 g) at 60 ^{o}C. Immediately after addition, the color of the solution changed from light green to dark-brown. The reaction mixture was allowed to stir for 3 h. The precipitate was collected by filtration, washed with methanol followed by ethyl ether, and air dried. The black-block single crystal appeared after about ten days of slow evaporation of mother liquor. Solubility: DMSO, DMF; Yield: 0.093 g, 62.0%. The solid product was identified as $[Co(C_{14}H_{12}O_3N_3)_2]$. Spectroscopic data of the complex were given as follows: 3026 cm^{-1} ($\nu_{C=C-H}$), 2834 cm^{-1} (ν_{C-H}), 1602 cm^{-1} ($\nu_{C=N}$), 1548, 1506 cm^{-1} ($\nu_{C=C}$), 1433 cm^{-1} ($\delta_{as\ C-H}$), 1241 cm^{-1}, 1212 cm^{-1} (ν_{Ph-O}), 737 cm^{-1}. Elemental analysis for $[Co(C_{14}H_{12}O_3N_3)_2]$, Calc. (Found): C 56.1 (56.0), H 4.0 (4.2), N 14.0 (13.8) %. ESI-MS (m/z): 599.9.

2.4. Computational details

The geometry optimization and frequency calculations of the dimer motif were performed in gas phase using the Gaussian 09 software package [21]. The starting geometry for the calculation was taken from the experimentally determined crystal structure. Geometrical optimization of Schiff base and its complex were carried out with the DFT B3LYP method [22,23]. We used the effective core potentials (ECPs) of Hav and Wadt with a double ζ-valence basis set LANL2DZ for the cobalt atoms [24], and the 6-31 G(d, p) basis sets for H, C, O, N atoms. Vibrational analyses were performed to ensure all stationary points to be local minima in the potential energy surfaces and no correction coefficient was used. The vibration bands were assigned by using Gauss View program.

2.5. Microcalorimetric measurement

The microcalorimetric experiments were determined on a TAM air isothermal microcalorimeter at 32 °C using the ampoule method. The principle and structure of the instrument were described in previous literature [20]. All 20-mL glass ampoules were cleaned and sterilized in high-pressure steam (0.1 MPa) at 120 °C before use. 5 mL YES culture medium containing S. pombe at the cell density of 1×10^6 colony-forming units (CFU)/mL was inoculated in a sterilized 20-mL glass ampoule, and then Schiff base and its complex at increasing concentrations were injected into each ampoule. All ampoules were sealed with special caps, shaken-up gently and placed in measuring channels. The metabolic power-time curves of S. pombe growth in the presence of two tested drugs were recorded in situ by a computer in a real-time manner.

2.6. X-ray single-crystal diffraction analysis

A single crystal of dimensions $0.13 \times 0.12 \times 0.1$ mm^3 for the complex was selected. Crystal data were collected with a SuperNova, Dual, Cu at zero, AtlasS2 diffractometer using monochromated Cu Ka radiation ($\lambda = 1.54184$) at 100.01(10) K. The crystal data were dealt with the program CrysAlisPro, Agilent Technologies Version 1.171.36.28 during data collection. The crystal displayed good diffraction quality and no variation in intensity during the course of data collection. A total of 29990 integrated reflections were collected, reducing to a data set of 10683 [R(int)=0.0994], and completeness of data to theta = 66.97° of 99.93%.

Using the program Olex2 [25], the structure was solved with the ShelXS structure solution program by direct methods and refined using full-matrix least-squares against F2 using SHELXL [26]. All non-hydrogen atoms were assigned anisotropic displacement parameters and refined without positional constraints. Hydrogen atoms were refined in geometrically idealized position with isotropic thermal parameters. The detailed crystallographic data and structure refinement parameters of the complex are summarized in Table 1. CCDC reference numbers: 2007789. Graphics were drawn with DIAMOND (Version 3.2) [27].

3. Results and discussion

3.1. The crystal structure of the complex

X-ray crystallographic analysis reveals that the complex crystallizes in the orthorhombic space group of Pbca symmetry. Its crystal structure consists of two symmetry-independent molecules (Fig. 1a). Two molecules are not only nearly identical in their distances and angles but also in their configuration. As shown in Fig. 1a, Co(II) ion is attached to the ligand in a ratio of 1:2. It is

six-coordinated to two azomethine nitrogen atoms, two carbonyl oxygen atoms and two phenolic oxygen atoms from two ligands. As depicted in Fig. 1b, Co(II) ion exhibits a slightly distorted octahedral configuration with two phenolic oxygen (O2 and O5), amide oxygen atom (O3 and O4) from two monoanion ligands consisting of the equatorial plane and two azomethine nitrogen atoms (N3 and N4) occupying the axial site. Selected bond lengths and angles are listed in Table 2. The Co–N bonds involved two azomethine nitrogen atoms were 1.866(6) Å and 1.865(6) Å, respectively. The Co–O bonds varied from 1.865(5) to 1.919(5) Å. The bond distances Co–N and Co–O in the complex are consistent with those reported in literatures [15,28]. Crystal packing of the complex is achieved by intramolecular and intermolecular hydrogen bonds. The hydrogen bond geometry is given in Table 1s. Hydrogen-bonds are formed between the oxygen atoms of methoxy or hydoroxy group and the hydrogen atoms of carbon atoms in the pyridine rings (Fig. 1s). Here, it should be noted that the oxidation sate of the cobalt has been verified to be +2 according to the XPS spectrum of the complex (Fig. 2s). This is because that there are seven 3d electrons in outermost shell of cobalt(II) and six electrons of cobalt(III). The cobalt(II) can provide more intense shake-up satellite in the high spin state, while cobalt(III) is diamagnetic and has no satellite peak [29].

3.2. Theoretical studies

3.2.1 Geometry optimization

The optimized molecular structures of Schiff base and its complex are shown in Fig. 2 and some selected structure parameters are shown in Table 2s. It should be pointed out that the phenol hydroxyl in Schiff base forms negative ion in the complex. Due to the instability of low spin state, the 3d electrons of Co^{2+} in the complex are in the weak electron field and high spin state. The calculated bond parameters are consistent with the experimental values, whereas the calculated bond length of cobalt ion with ligand and the torsion angle of pyridine ring deviates from experimental values. These deviations may be caused by the strong intermolecular force. The pyridine ring in the complex crystal is almost coplanar with the other groups due to the intermolecular π-π stack. In the gas phase, the intramolecular repulsive force leads to the pyridine ring departure from the conjugate plane, with the torsion angle about 26°.

The most important orbitals in a molecule are the frontier molecular orbitals. The frontier molecular orbitals for the closed shell molecule include the highest occupied molecular orbital (HOMO) and the lowest unoccupied molecular orbital (LUMO). While for the open shell molecules, the HOMO may be singly occupied molecular orbitals (SOMO). The HOMO of Schiff base mainly comes from the lone electron pair of oxygen atom, as shown in Fig. 3. The LUMO mainly locate at the π* anti-bond orbital of C-N bond in the pyridine ring. The formed energy gap between HOMO

and LUMO indicates the molecular chemical stability. Molecules which have a large HOMO-LUMO energy gap maybe called hard and which have a small energy gap maybe called soft [30]. The calculated band gap for Schiff base is 4.05 eV, which means good stability and a high chemical hardness for Schiff base. But the calculated band gap for the complex is only 2.64 eV.

3.2.2 Vibrational assignments

The experimental and theoretical IR spectra of the complex in 400-4000 cm^{-1} region are shown in Fig. 4. The vibrational wavenumbers were calculated according to the optimized geometries in gas phase by using B3LYP method with the basis set. It is noted that none of the frequency calculations is found to exhibit any imaginary frequency, which is consistent with an energy minimum for the optimized geometry that proves the reliability of the obtained results. The peaks at 1602 cm^{-1} is a coupled vibration coming from azomethine group (C=N) and carbonyl group (C=O), were calculated at 1665 cm^{-1} for the complex. The peak of at 1548 cm^{-1}, 1506 cm^{-1} for C=C ring stretch of aromatic groups, the calculated peak is located at 1593 cm^{-1}, 1575 cm^{-1}. The asymmetric stretching vibration of C-H bond appears at 1433 cm^{-1}, while the corresponding theoretical value is 1492 cm^{-1}. The absorption at 1241 cm^{-1}, 1212 cm^{-1} for the phenolic oxygen group (Ph-O), the calculated value is recorded in 1284 cm^{-1}, 1243 cm^{-1}.

3.3. Microcalorimetry

3.3.1 The normal metabolic power–time curve of S. pombe

The metabolic power–time curve of S. pombe growth at 32 °C in the absence of tested drug is shown in Fig. 5a. As S. pombe was inoculated in YES culture medium under isochoric conditions and limited nutrients and oxygen, the metabolic process could be divided into four phases, namely, a lag phase (AB), a log(exponential) phase (BC), a stationary phase (CD) and a decline phase (DE). During the log phase, the power–time curves could obey the following equation [31]:

$$P_t = P_0 \exp[k(t-t_0)]$$

or

$$\ln P_t = \ln P_0 + kt - kt_0$$

The above equations are called biothermokinetic equation of growth metabolic of S. pombe, where P_0 and P_t stand for the heat–output power at initial time t = 0 and any time t, respectively. k is the growth rate constant for S. pombe at specified condition. The growth rate constant k of the exponential phase was calculated by fitting $\ln P_t$ and t to a linear equation.

3.3.2 Metabolic power–time curves of S. pombe affected by Schiff base and its complex

When the suspensions of S. pombe were introduced into the ampoules with different concentrations of tested drugs, there existed corresponding changes in the power–time curves. As presented in Fig. 5b and 5c, compared with the blank control group, the height, peak time and shape of each experimental group were significantly changed. From the metabolic power–time curves of S. pombe growth, four quantitative thermokinetic parameters (k, P, t_G and Q) were obtained and are illustrated in Table 3. In comparison with the control, k, P and Q decreased and t_G increased with the increase of drug concentration. The inhibition ratio (I) of the growth metabolism of S. pombe by the tested drugs could be descried as the following equation:

$$I = \frac{(k_0 - k_c)}{k_0} \times 100\%$$

Where k_0 is the rate constant of the control and k_c is the rate constant under an inhibitor with a concentration of c. When the inhibition ratio (I) is 50%, the corresponding concentration of inhibitor is called as the half inhibition concentration IC_{50}. To explore the inhibitory effect of the tested drugs on S. pombe, the values of I and IC_{50} were calculated. As are shown in Table 3, the half inhibition concentration (IC_{50}) of Schiff base and its complex are 1.18×10^{-2} mol L^{-1} and 1.07×10^{-3} mol L^{-1}, respectively, which indicates the complex has a stronger inhibition effect than that of Schiff base on S. pombe growth. It is possible that the biological activity of the complex is not only related to the structure of the ligand, but also depends on the property of the central metal ion [32].

3.3.3 Quantitative relationship between thermokinetic parameters and concentrations of Schiff base and its complex.

3.3.3.1 Relationship between I and C

Plotting the inhibition ratio (I) against the concentration (c) of Schiff base and its complex, Fig. 3s was obtained. According to Fig. 3s, when the concentration of the tested drugs increased, I values increased gradually, which reveals that both Schiff base and its complex have inhibition effect on S. pombe growth. Using the Logistic curve fitting from data of I and c, the I-c equations could be described in Eqs. (1) and (2) (see Table 4):

3.3.3.2 Relationship between k and c

Drawing the inhibition ratio (k) of S. pombe growth against concentration (c), the corresponding curves are shown in Fig.4s. Fig. 4s illustrated that as the concentrations of the tested drugs increased, the growth rate constant (k) of S. pombe decreased. The quantitative relationship between k and c by nonlinear fitting were given in Eqs. (3) and (4) (see Table 4):

3.3.3.3 Relationship between P_{max} and c

The P_{max}-c curves were drawn relied on the maximum heat-output power (P_{max}) and the different concentration (c) of the tested drugs. As presented in Fig. 5s, as the concentration of the tested drugs increased, the P_{max} of S. pombe decreased. The P_{max}-c equations were shown in Eqs. (5) and (6) of Table 4 by using the nonlinear fitting method, in which the correlation coefficients R of Schiff base and its complex were 0.9843 and 0.9935, respectively.

3.3.3.4 Relationship between t_G and c

As the biothermokinetic equation was very similar to the indefinite integral relation of rate equation of the first order reaction, the mathematical expression of generation time (t_G) of S. pombe was defined by simulating the relationship between the half-life of the first order reaction and the rate constant of the reaction. The generation time (t_G) of the growth metabolism S. pombe treated by drugs was defined as follows:

$t_{G=}$ ln2/k

where t_G was generation time and k was growth rate constant of S. pombe. The t_G of S. pombe were calculated at different concentration of the tested drugs, as summarized in Table 3. The t_G-c curves were drawn from t_G and c. As could be seen from Fig. 6s, the generation time (t_G) of S. pombe increased with the increasing concentration of the tested drugs. The t_G-c equations were produced by using the nonlinear fitting method (see Eqs. (7) and (8) in Table 4)

3.3.3.5 Relationship between Q_{total} and c

Plotting the total heat-output (Q_{total}) against the concentration (c), the curves were illustrated in Fig. 7s. As shown in Fig. 7s, with the increase of the concentrations of the tested drugs, the Q_{total} of S. pombe decreased. Using the logistic curve fitting from data of the the total heat-output (Q_{total}) of S. pombe growth against concentration (c), the Q_{total}-c equations were produced (as shown in Eqs. (9) and (10) of Table 4). The correlation coefficients R of Schiff base and its complex were 0.9671 and 0.9890, respectively.

4. Conclusions

In conclusion, a new cobalt(II) Schiff-base complex has been synthesized and characterized. X-ray crystallographic analysis revealed that a cobalt(II) was coordinated by two Schiff-base ligands via azomethine, carbonyl oxygen atoms and phenolic oxygen atoms. DFT calculations have been done for Schiff base and its complex. Their calculated band gaps are 4.05 eV and 2.64 eV,

respectively, which means Schiff base has good stability and a high chemical hardness. They have also been screened for their antibacterial (S. pombe) by bio-microcalorimetry. The antibacterial test referred that the complex recorded significant inhibition efficiency against S. pombe than Schiff base. According to the metabolic power–time curves, some thermokinetic parameters were obtained, and their quantitative relationship with the concentration were discussed. As a basic research, the purpose of this study is to afford some valuable reference data for further study of Schiff bases and their complexes.

Acknowledgements

The authors thank The National Natural Science Foundation of China (No. 21273190), The Hunan Provincial Natural Science Foundation of China (No. 2017JJ2240), The Project of Scientific Research of Hunan Provincial Education Department (No. 18B499, 20A463), The Hunan University Students' Innovation and Entrepreneurship Training Program Project (No. S202010545008) and Science and Technology Plan Project of Chenzhou city (No. ZDYF2020154) for financial support.

Appendix A. Supplementary data

CCDC 2007789 contains the supplementary crystallographic data for the complex. These data can be obtained free of charge via http://www.ccdc.cam.ac.uk/conts/retrieving.html, or from the Cambridge Crystallographic Data Centre, 12 Union Road, Cambridge CB2 1EZ, UK; fax: (+44) 1223-336-033; or e-mail: deposit@ccdc.cam.ac.uk.

References

[1] X. Liu, J.R. Hamon, Recent developments in penta-, hexa- and heptadentate Schiff base ligands and their metal complexes, Coord. Chem. Rev. 389 (2019) 94-118.

[2] V.B. Badwaik, R.D. Deshmukh, A.S. Aswar, Transition metal complexes of a Schiff base: synthesis, characterization, and antibacterial studies, J. Coord. Chem. 62 (2009) 2037-2047.

[3] D. Sinha, A.K. Tiwari, S. Singh, G. Shukla, P. Mishra, H. Chandra, A.K. Mishra, Synthesis, characterization and biological activity of Schiff base analogues of indole-3-carboxaldehyde, Eur. J. Med. Chem. 43 (2008) 160-165.

[4] S. Adsule, V. Barve, D. Chen, F. Ahmed, Q.P. Dou, S. Padhye, F.H. Sarkar, Novel Schiff base copper complexes of quinoline-2 carboxaldehyde as proteasome inhibitors in human prostate cancer cells, J. Med. Chem. 49 (2006) 7242-7246.

[5] S. Ren, R. Wang, K. Komatsu, P. Bonaz-Krause, Y. Zyrianov, C.E. McKenna, C. Csipke, Z.A. Tokes, E.J. Lien, Synthesis, biological evaluation, and quantitative structure-activity relationship analysis of new Schiff bases of hydroxysemicarbazide as potential antitumor Agents, J. Med. Chem. 45 (2002) 410-419.

[6] A.K. Ghosh. M. Mitra, A. Fathima, H. Yadav, A.R. Choudhury, B.U. Nair, R. Ghosh, Antibacterial and catecholase activities of Co(III) and Ni(II) Schiff base complexes, Polyhedron 107 (2016) 1-8

[7] C.R. Krishna Murti, Isonicotinic acid hydrazide, in: J.W. Corcoran, F.E. Hahn, J.F. Snell, K.L. Arora (Eds.), Mechanism of action of antimicrobial and antitumor agents, Springer-Verlag Berlin Heidelberg, 1975, pp. 623-652.

[8] S. Somasundaram, A. Ram, L. Sankaranarayanan, isoniazid and rifampicin as therapeutic regimen in the current era: a review, Journal of Tuberculosis Research, 2 (2014) 40-51.

[9] B.F. Lei, C.J. Wei, Action mechanism of antitubercular isoniazid, The Journal of Biological Chemistry, 275 (2000) 2520-2526.

[10] E.N. Mainsah, P.T. Ndifon, E.N. Nfor, J.N. Njapba, Synthesis, characterization and antibacterial properties of some transition metal complexes of (1H-pyrrol-2-yl)isonicotinoyl hydrazine, Bull. Chem. Soc. Ethio. 27 (2013) 395-404.

[11] O. Berkesi, T. Kortvelyesi, C. Hetenyi, T. Nemeth, I. Palinko, Hydrogen bonding interaction of benzylidene type Schiff bases studied by vibrational spectroscopic and computational methods, Phys. Chem. Chem. Phys. 5 (2003) 2009-2014.

[12] L. Habala, S. Varenyi, A. Bilkova, P. Herich, J. Valentova, J. Kozisek, F. Devinsky, Antimicrobial activity and urease inhibition of Schiff bases derived from isoniazid and fluorinated benzaldehydes and of their copper(II) complexes, Molecules 21 (2016) 1742.

[13] E.N. Mainsah, S.J.E. Ntum, M. Samje, F. Chongwa, P.T. Ndifon, J.N Yong, Synthesis and anti-onchocercal activity of isonicotinoyl hydrazones and their copper(II) and zinc(II) complexes, Anti-Infective Agents. 14 (2016) 47-52.

[14] J. Xu, Synthesis, crystal structure, and antibacterial activity of N′-(2-hydroxy-3-methoxybenzylidene)isonicotinohydrazide and its dinuclear manganese(II) complex with N′-(2-hydroxy-3-methoxybenzylidene)isonicotinohydrazide, Synth. React. Inorg. M. 43 (2013) 1329-1333.

[15] M. Tabatabae, A. Taghinezhadkoshknou, M. Dusek, K. Fejfarova, Synthesis and characterization of a cobalt(II) complex with (E)-N'-(2-hydroxy-3-methoxybenzylidene) isonicotinohydrazide and (E)-N'-(2-hydroxy-3-methoxybenzylidene)isonicotinohydrazidanium nitrate as a by-product, Synth. React. Inorg. M. 45 (2015) 1506-1512.

[16] C.H. Li, J.H. Jiang, X. Li, L.M. Tao, S.X. Xiao, H.W. Gu, H. Zhang, C. Jiang, J.Q. Xie, M.N. Peng, L.L. Pan, X.M. Xia, Q.G. Li, Synthesis, crystal structure and biological properties of a bismuth(III) Schiff-base complex, RSC Adv. 5 (2015) 94267-94275.

[17] C.H. Li, J.H. Jiang, P. Yang, X. Li, S.X. Xiao, X. Tao, J.Q. Xie, Q.G Li, Preparation, structure and thermochemical properties of a copper(II) Schiff-base complex, J. Therm. Anal. Calorim. 119 (2015) 1285-1292.

[18] J.Q. Xie, C.H. Li, J.X. Dong, W. Qu, L. Pan, M.L. Peng, M.A. Xie, X. Tao, C.M. Yu, Y. Zhu, P.H. Zhang, C.G. Tang, Q.G. Li, The standard molar enthalpy of formation of a new copper(II) Schiff-base complex and its interaction with bovine serum albumin, Thermochim. Acta 589 (2014) 7-15.

[19] C.H. Li, X.Z. Song, J.H. Jiang, H.W. Gu, L.M. Tao, P. Yang, X. Li, S.X. Xiao, F.H. Yao, W.Q. Liu, J.Q. Xie, M.N. Peng, L. Pan, X.B. Wu, C. Jiang, S. Wang, M.F. Xu, Q.G. Li, Synthesis, crystal structure and thermodynamic properties of a new praseodymium Schiff-base complex, Thermochim. Acta 581 (2014) 118-122.

[20] X. Li, J.H. Jiang, Q.Q. Chen, S.X. Xiao, C.H. Li, H.W. Gu, H. Zhang, J.L. Hu, F.H. Yao, Q.G. Li, Synthesis of nordihydroguaiaretic acid derivatives and their bioactivities on S. pombe and K562 cell lines, Eur. J. Med. Chem. 62 (2013) 605-613.

[21] M.J. Frisch, G.W. Trucks, H.B. Schlegel, G.E. Scuseria, M.A. Robb, J.R. Cheeseman, G. Scalmani, V. Barone, B. Mennucci, G.A. Petersson, H. Nakatsuji, M. Caricato, X. Li, H.P. Hratchian, A.F. Izmaylov, J. Bloino, G. Zheng, J. L. Sonnenberg, M. Hada, M. Ehara, K. Toyota, R. Fukuda, J. Hasegawa, M. Ishida, T. Nakajima, Y. Honda, O. Kitao, H. Nakai, T. Vreven, J.A. Montgomery, Jr., J.E. Peralta, F. Ogliaro, M. Bearpark, J.J. Heyd, E. Brothers, K.N. Kudin, V.N. Staroverov, T. Keith, R. Kobayashi, J. Normand, K. Raghavachari, A. Rendell, J.C. Burant, S.S. Iyengar, J. Tomasi, M. Cossi, N. Rega, J.M. Millam, M. Klene, J.E. Knox, J.B. Cross, V. Bakken, C. Adamo, J. Jaramillo, R. Gomperts, R.E. Stratmann, O. Yazyev, A.J. Austin, R. Cammi, C. Pomelli, J.W. Ochterski, R.L. Martin, K. Morokuma, V.G. Zakrzewski, G. A. Voth, P. Salvador, J.J. Dannenberg, S. Dapprich, A.D. Daniels, O. Farkas, J.B. Foresman, J.V. Ortiz, J. Cioslowski, D.J. Fox, Gaussian 09, Revision B. 01, Gaussian Inc., Wallingford CT, 2010.

[22] C. Lee, W. Yang, R.G. Parr, Development of the Colle-Salvetti correlation-energy formula into a functional of the electron density, Phys. Rev. B 37 (1988) 785-789.

[23] A.D.J. Becke, Density-functional thermochemistry. III. The role of exact exchange, J. Chem. Phys. 98 (1993) 5648-5652.

[24] M. Couty, M.B. Hall, Basis sets for transition metals: optimized outer p functions. J. Comput.

Chem. 17 (1996) 1359-1370.

[25] O.V. Dolomanov, L.J. Bourhis, R.J. Gildea, J.A.K. Howard, H. Puschmann, OLEX2: a complete structure solution, refinement and analysis program, J. Appl. Crystallogr. 42 (2009) 339-341.

[26] G.M. Sheldrick, A short history of SHELX, Acta. Crystallogr. A 64 (2008) 112-122.

[27] K. Brandenburg, Diamond (Version 3.2), Crystal and Molecular Structure Visualization, Germany, 2009, http://www.crystalimpact.com/diamon.

[28] E. Gungor, S. Celen, D. Azazb, H. Kara, Two tridentate Schiff base ligands and their mononuclear cobalt (III) complexes: synthesis, characterization, antibacterial and antifungal activities, Spectrochim. Acta Part A. 94 (2012) 216-221.

[29] J.A. Sans, J.F. Sanchez-Royo, J. Pellicer-Porres, A. Segura, E. Guillotel, G. Martinez-Criado, J. Susini, A. Munoz-Paez, V. Lopez-Flores, Optical, X-ray absorption and photoelectron spectroscopy investigation of the Co site configuration in $Zn_{1-x}Co_xO$ films prepared by pulsed laser deposition, Superlattices and Microstructures. 42 (2007) 226-230.

[30] E.F. Silva-Júnior, D.L. Silva, P.F.S. Santos-Júnior, I.J.S. Nascimento, S.W.D. Silva, T.L. Balliano, T.M. Aquino, J.X. Araújo-Júnior, Crystal structure and DFT calculations of 4,5-dichloropyridazin-3-(2H)-one, J. Chem. Pharm. Res. 8 (2016) 279-286.

[31] C.L. Xie, H.K. Tang, Z.H. Song, S.S. Qu, Y.T. Liao, H.S. Liu, Microcalorimetric study of bacterial growth, Thermochim. Acta 123 (1988) 33-41.

[32] X. Li, C.H. Li, J.H. Jiang, H.W. Gu, D.L. Wei, L.J. Ye, J.L. Hu, S.X. Xiao, D.C. Guo, X. Li, H. Zhang, Q.G. Li, Synthesis and microcalorimetric determination of the bioactivities of a new Schiff base and its bismuth(III) complex derived from o-vanillin and 2,6-pyridinediamine, J. Therm. Anal. Calorim. 127 (2017) 1767-1776.

Legends to Figures

Fig. 1 (a) Molecular structure of the complex. **(b)** Coordination polyhedron of Co(II) ion in the complex.

Fig. 2 Theoretical structure of **(a)** Schiff base and **(b)** the complex.

Fig. 3 The frontier orbit of Schiff base and the complex. **(a)** HOMO of Schiff base. **(b)** LUMO of Schiff base. **(c)** SOMO of the complex. **(d)** LUMO of the complex.

Fig. 4 Experimental and theoretical IR spectra of the complex.

Fig. 5 Metabolic power-time curves of S. pombe cells affected by the tested drugs at 32.00 °C. **(a)** for control. **(b)** Schiff base. **(c)** the complex.

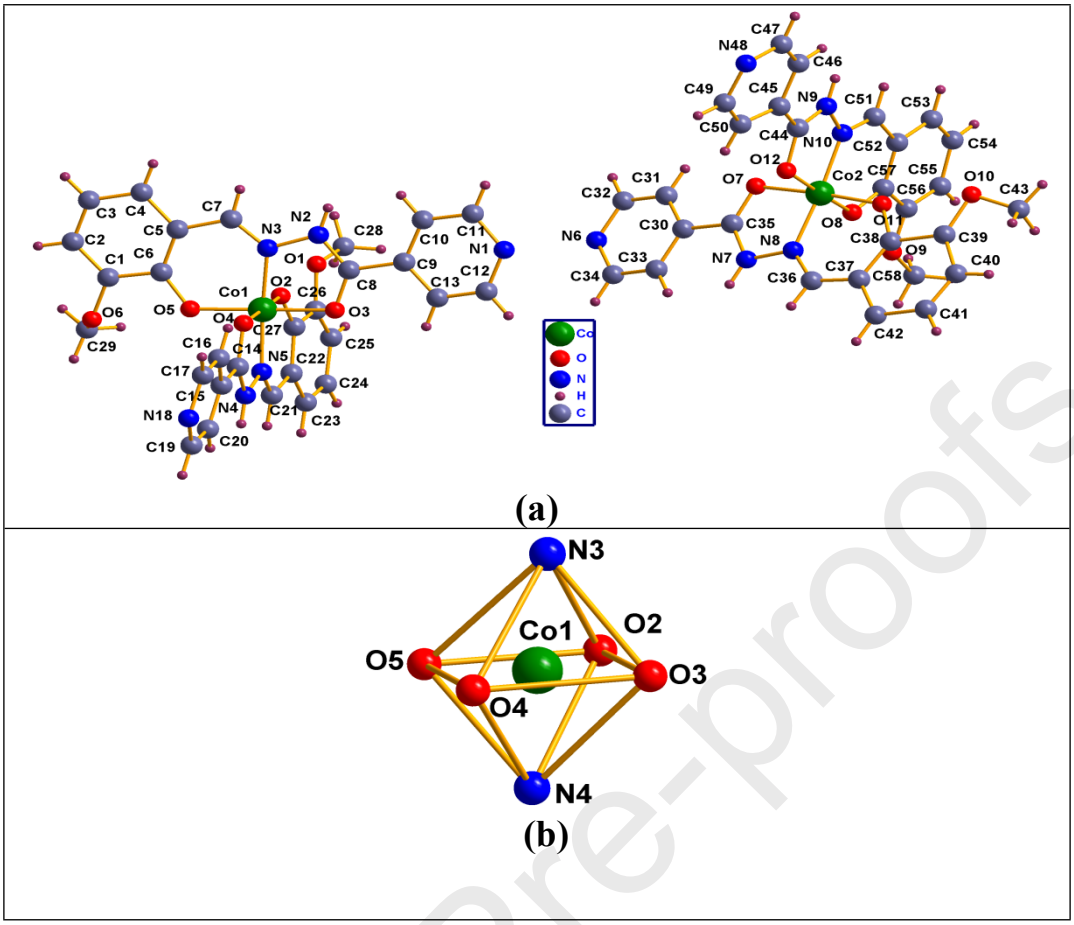

Fig. 1 (a) Molecular structure of the complex. **(b)** Coordination polyhedron of Co(II) ion in the complex.

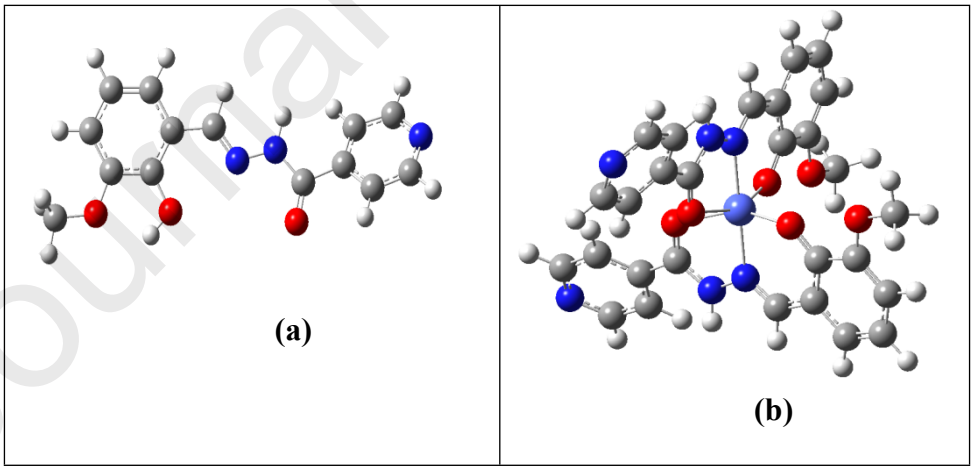

Fig. 2 Theoretical structure of **(a)** Schiff base and **(b)** the complex.

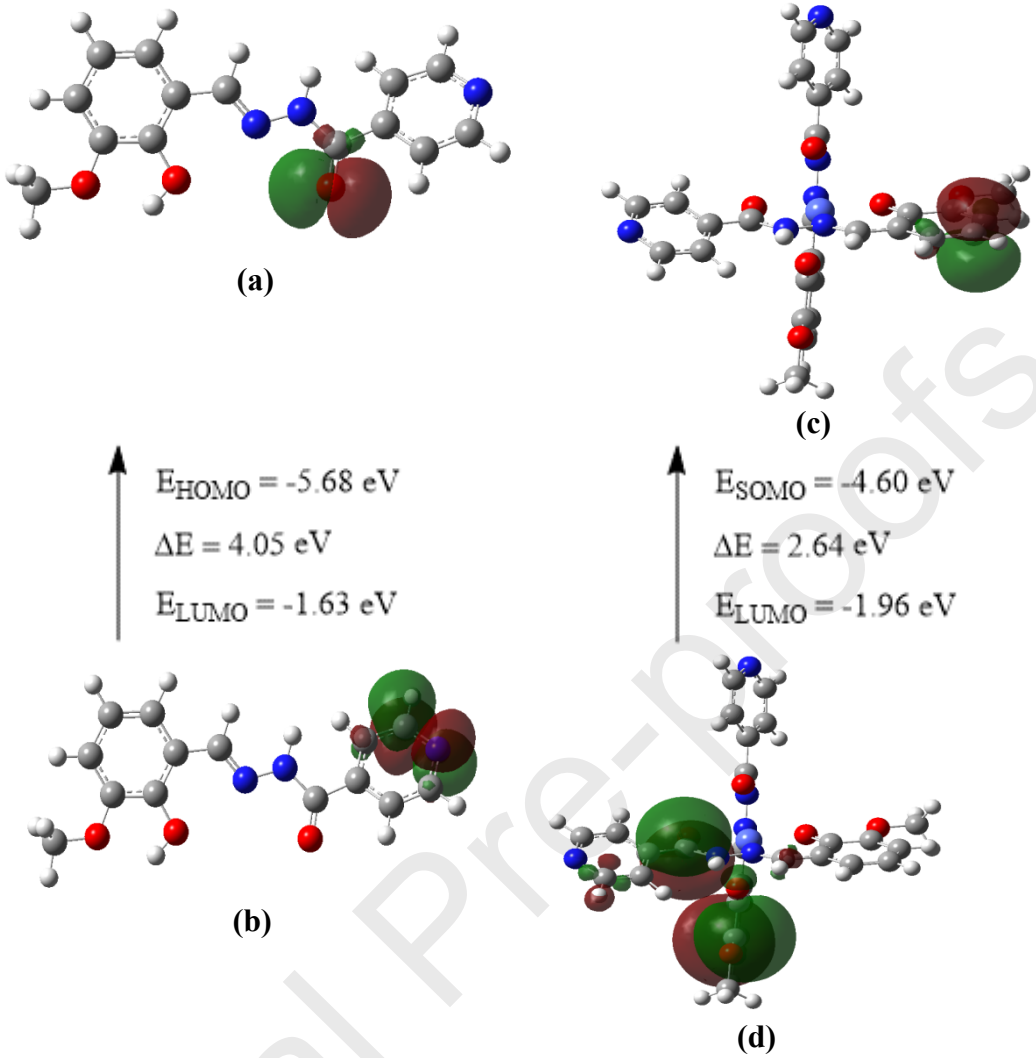

Fig. 3 The frontier orbit of Schiff base and the complex. **(a)** HOMO of Schiff base. **(b)** LUMO of Schiff base. **(c)** SOMO of the complex. **(d)** LUMO of the complex.

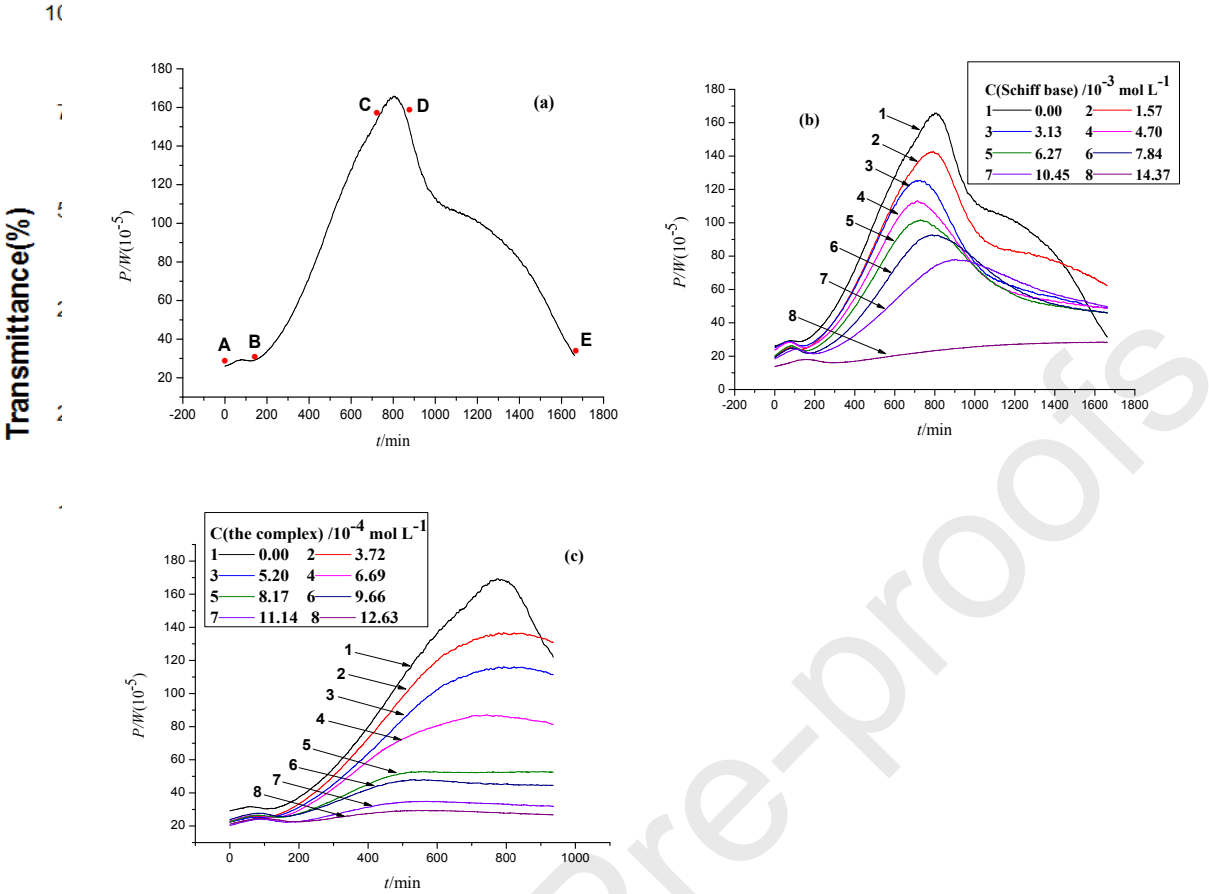

Fig. 4 Experimental and theoretical IR spectra of the complex.

Fig. 5 Metabolic power-time curves of S. pombe cells affected by the tested drugs at 32.00 °C. (**a**) for control. (**b**) Schiff base. (**c**) the complex.

Legends to Tables

Table 1 Crystallographic data for the complex.

Table 2 Selected bond lengths (Å) and bond angles (°) for the complex.

Table 3 Thermokinetic parameters of the growth of S. pombe affected by different concentrations of Schiff base and its complex at 32 ^{o}C.

Table 4 Quantitative relationship between thermokinetic parameters and concentrations of Schiff base and its complex.

Table 1
Crystallographic data for the complex.

Crystal data

CCDC No.	2007789	Z	16
Empirical formula	$C_{28}H_{24}CoN_6O_6$	Dcalc (g/cm^3)	1.466
Formula weight	599.46	Absorption coefficient (mm^{-1})	5.420
Temperature (K)	100.01(10)	Crystal size (mm)	0.13 × 0.12 × 0.1
Wavelength (Å)	1.54184	Reflections collected	29990
Crystal system	orthorhombic	Independent reflections (Rint)	10683
Space group	Pbca	Completeness to theta =66.97° (%)	99.93 %
a (Å)	19.1448(18)	2Θ range for data collection/°	5.214 -147.526
b (Å)	16.7388(12)	h, k, l range	-23 ≤ h ≤ 23, -20 ≤ k ≤ 11, -31 ≤ l ≤ 41
c (Å)	33.892(4)	Data/restraints/parameters	10683/54/743
α (°)	90	Goodness-of-fit on F^2	1.036
β (°)	90	Final R indices [I > 2σ(I)]	R_1 = 0.0912, wR_2 = 0.2380
γ (°)	90	R indices (all data)	R_1 = 0.1630, wR_2 = 0.2930
V (Å^3)	10861.1(18)		

Table 2
Selected bond lengths (Å) and bond angles (°) for the complex.

Bond distances (Å)				
Co(1)–O(2)	1.865(5)	Co(1)–N(3)	1.866(6)
Co(1)–O(3)	1.903(5)	Co(1)–N(4)	1.865(6)
Co(1)–O(4)	1.919(5)	C(14)–O(4)	1.298(8)
Co(1)–O(5)	1.886(4)	C(8)–O(3)	1.278(8)
Bond angles (°)			
O(2)–Co(1)–O(3)	90.4(2)	N(3)–Co(1)–O(3)	83.4(2)
O(2)–Co(1)–O(4)	179.7(2)	N(3)–Co(1)–O(4)	92.9(2)
O(2)–Co(1)–O(5)	90.4(2)	N(3)–Co(1)–O(5)	95.9(2)
O(2)–Co(1)–N(3)	87.3(2)	N(4)–Co(1)–O(3)	91.9(2)
O(2)–Co(1)–N(4)	96.2(3)	N(4)–Co(1)–O(4)	83.6(2)
O(3)–Co(1)–O(4)	89.9(2)	N(4)–Co(1)–O(5)	88.7(2)
O(5)–Co(1)–O(3)	179.0(2)	N(4)–Co(1)–N(3)	174.2(2)
O(5)–Co(1)–O(4)	89.3(2)		

Table 3
Thermokinetic parameters of the growth of S. pombe affected by different concentrations of Schiff base and its complex at 32 °C.

Drugs	C[a]/ mol L^{-1}	k[b]/s^{-1}	R	I[c]/%	IC$_{50}$[d]/ mol L^{-1}	P$_{max}$[e]/ W	t$_G$[f]/s	Q$_{total}$[g]/ J
Schiff base	0	5.54×10^{-5}[h] ± 7.57×10^{-8}	0.9956	0	**1.18×10^{-2}**	1.65×10^{-3}	1.25×10^{4}	59.07
	1.57×10^{-3}	5.34×10^{-5} ± 9.85×10^{-8}	0.9907	3.68		1.43×10^{-3}	1.30×10^{4}	38.41
	3.13×10^{-3}	5.23×10^{-5} ± 9.31×10^{-8}	0.9919	5.55		1.26×10^{-3}	1.32×10^{4}	31.31
	4.70×10^{-3}	5.15×10^{-5} ± 7.96×10^{-8}	0.9940	7.04		1.13×10^{-3}	1.35×10^{4}	27.33
	6.27×10^{-3}	4.93×10^{-5} ± 8.76×10^{-8}	0.9919	10.99		1.02×10^{-3}	1.41×10^{4}	25.50
	7.84×10^{-3}	4.53×10^{-5} ± 7.07×10^{-8}	0.9932	18.33		9.28×10^{-4}	1.53×10^{4}	23.45
	1.045×10^{-2}	3.50×10^{-5} ± 5.88×10^{-8}	0.9912	36.88		7.78×10^{-4}	1.98×10^{4}	18.06
	1.437×10^{-2}	1.13×10^{-5} ± 1.74×10^{-8}	0.9916	79.56		2.84×10^{-4}	6.12×10^{4}	1.52
the complex	0	5.26×10^{-5} ± 7.31×10^{-8}	0.9922	0	**1.07×10^{-3}**	1.69×10^{-3}	1.32×10^{4}	15.10
	3.72×10^{-4}	4.97×10^{-5} ± 9.69×10^{-8}	0.9839	5.39		1.36×10^{-3}	1.39×10^{4}	7.22
	5.20×10^{-4}	4.81×10^{-5} ± 7.55×10^{-8}	0.9901	8.55		1.16×10^{-3}	1.44×10^{4}	6.35
	6.69×10^{-4}	4.51×10^{-5} ± 1.00×10^{-8}	0.9832	14.30		8.72×10^{-4}	1.54×10^{4}	6.14
	8.17×10^{-4}	3.79×10^{-5} ± 5.09×10^{-8}	0.9955	27.88		5.25×10^{-4}	1.83×10^{4}	3.41
	9.66×10^{-4}	3.15×10^{-5} ± 5.82×10^{-8}	0.9908	40.01		4.79×10^{-4}	2.20×10^{4}	3.10
	1.114×10^{-3}	2.38×10^{-5} ± 4.38×10^{-8}	0.9916	54.74		3.48×10^{-4}	2.91×10^{4}	1.98

	1.263×10^{-3}	$1.55\times10^{-5}\pm3.27\times10^{-8}$	0.9902	70.53		2.93×10^{-4}	4.47×10^{4}	1.22

[a] The concentration
[b] The growth rate constant of S. pombe
[c] The inhibition ratio
[d] The half inhibition concentration
[e] The maximum heat-output power
[f] The generation time
[g] The total heat-output
[h] Mean ± S.D.; n = 3

Table 4 Quantitative relationship between thermokinetic parameters and concentrations of Schiff base and its complex.

$$z = \mathrm{A} + \frac{\mathrm{B}}{1+(\frac{c}{\mathrm{D}})^{\mathrm{m}}}$$

z	A	B	D	m	R	Serial number
I	27363.23	–27360.95	142.93	2.55	0.9982	(1)[a]
	205.33	–204.50	1.58	2.92	0.9985	(2)[b]
k	–1510.54	1515.96	142.92	2.55	0.9982	(3)[a]
	–5.54	10.75	1.58	2.92	0.9985	(4)[b]
$\mathbf{P_{max}}$	–59957.06	59958.68	2.11×10^{-6}	0.90	0.9843	(5)[a]
	0.09	1.59	0.64	2.93	0.9935	(6)[b]
$\mathbf{t_G}$	2041.00	–2039.67	38.72	6.10	0.9992	(7)[a]
	8905.50	–8904.10	6.12	5.06	0.9971	(8)[b]
$\mathbf{Q_{total}}$	–31275.67	31333.95	8.37×10^{6}	0.48	0.9671	(9)[a]
	–1404.74	1419.81	95682.13	0.52	0.9890	(10)[b]

Note: **z** refers to thermokinetic parameters (**I, k,** $\mathbf{P_{max}}$, $\mathbf{t_G}$ and $\mathbf{Q_{total}}$).
c refers to the concentration.
R is correlation coefficient.
[a] For Schiff base, 0.00 mol $L^{-1} \le c_{\text{Schiff base}} \le 1.44\times10^{-2}$ mol L^{-1}.
[b] For the complex, 0.00 mol $L^{-1} \le c_{\text{the complex}} \le 1.26\times10^{-3}$ mol L^{-1}.

Graphical Abstract

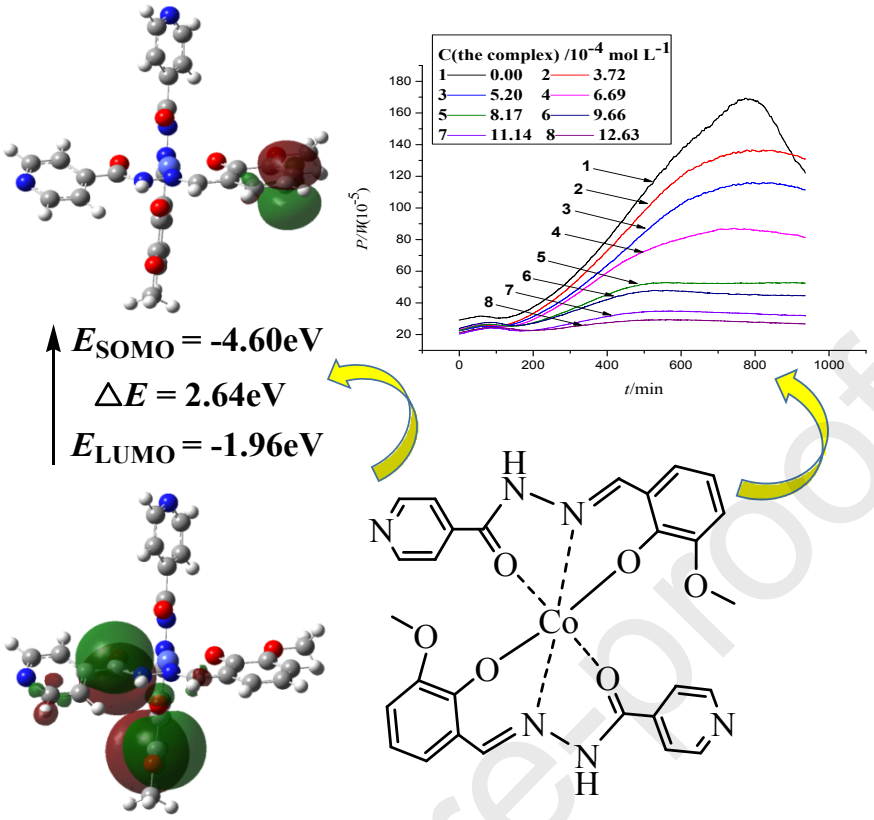

Highlights

- A new cobalt(II) complex was synthesized and characterized.
- Theoretical studies using DFT calculations.
- The bioactivity of cobalt(II) complex was assessed by bio-microcalorimetry.
- The complex displayed much stronger antibacterial activity than Schiff base.
- Some thermokinetic parameters (k, P_{max}, t_G and Q_{total}) were derived.

Credit Author Statement

Jian-Hong Jiang: Methodology, Validation. **Yan-Hua Lei:** Formal analysis, Validation. **Xu Li:** Visualization. **Yiyuan Pi:** Writing-Original Draft. **He Zhu:** Investigation. **Qiang-Guo Li:** Resources, Funding acquisition, Project administration, Writing-review & editing. **Chuan-Hua Li:** Conceptualization, Methodology, Writing-review & editing, Data curation.

Declaration of interests

☒ The authors declare that they have no known competing financial interests or personal relationships that could have appeared to influence the work reported in this paper.

☐The authors declare the following financial interests/personal relationships which may be considered as potential competing interests: